

Solar energetic particles in the Heliosphere

Dalmiro Jorge Filipe Maia

CICGE, Centro de Investigação em Ciências Geo-espaciais

Faculdade de Ciências da Universidade do Porto, Portugal

Partially support by FCT (Fundação para a Ciência e Tecnologia) through grant PEst-OE/CTE/UI0190/2011.

FCT Fundação para a Ciência e a Tecnologia
MINISTÉRIO DA EDUCAÇÃO E CIÊNCIA


COMPETE
Programa Operacional Competitividade e Inovação


QR
QUADRO DE REFERÊNCIA
ESTRATÉGICO
NACIONAL
2007-2013


GOVERNO DA REPÚBLICA
PORTUGUESA


UNIÃO EUROPEIA
Fundo Social Europeu

Particles in the heliosphere

In situ particle observations can be attributed to a series of particle populations, whose relative importance and local characteristics vary widely from solar maximum to solar minimum. Energetic particle populations in the inner heliosphere include:

Particles in the heliosphere

In situ particle observations can be attributed to a series of particle populations, whose relative importance and local characteristics vary widely from solar maximum to solar minimum. Energetic particle populations in the inner heliosphere include:

1. Galactic cosmic Rays (GCRs) originated in the interstellar medium and able to penetrate into the heliosphere.

Particles in the heliosphere

In situ particle observations can be attributed to a series of particle populations, whose relative importance and local characteristics vary widely from solar maximum to solar minimum. Energetic particle populations in the inner heliosphere include:

1. Galactic cosmic Rays (GCRs)
2. Anomalous cosmic rays (ACRs), that originate as interstellar neutral atoms traveling into the heliosphere, ionized by solar UV and carried out as pickup ions in the solar wind to be finally accelerated to energies as high as 100 MeV/nucleon presumably close to the solar wind termination shock or in the heliosheath.

Particles in the heliosphere

In situ particle observations can be attributed to a series of particle populations, whose relative importance and local characteristics vary widely from solar maximum to solar minimum. Energetic particle populations in the inner heliosphere include:

1. Galactic cosmic Rays (GCRs)
2. Anomalous cosmic rays (ACRs)
3. Solar energetic particles (SEPs) that originate near the Sun in association with intense solar flares and large coronal mass ejections (CMEs). Occasionally, SEP events are observed at very high energies reaching GeV for protons and 100 MeV for electrons.

Particles in the heliosphere

In situ particle observations can be attributed to a series of particle populations, whose relative importance and local characteristics vary widely from solar maximum to solar minimum. Energetic particle populations in the inner heliosphere include:

1. Galactic cosmic Rays (GCRs)
2. Anomalous cosmic rays (ACRs)
3. Solar energetic particles (SEPs)
4. Energetic particles accelerated by other shocks and disturbances in the solar wind such as shocks formed in the solar wind stream interaction regions (SIRs) or corotating interaction regions (CIRs).

Particles in the heliosphere

In situ particle observations can be attributed to a series of particle populations, whose relative importance and local characteristics vary widely from solar maximum to solar minimum. Energetic particle populations in the inner heliosphere include:

1. Galactic cosmic Rays (GCRs)
2. Anomalous cosmic rays (ACRs)
3. Solar energetic particles (SEPs)
4. Particles accelerated by SIRs or CIRs
5. Energetic particles accelerated in planetary magnetospheres, such as Jovian electrons observed in the inner heliosphere at energies from a few hundred keV to less than about 30 MeV.

Particles in the heliosphere

In situ particle observations can be attributed to a series of particle populations, whose relative importance and local characteristics vary widely from solar maximum to solar minimum. Energetic particle populations in the inner heliosphere include:

1. Galactic cosmic Rays (GCRs)
2. Anomalous cosmic rays (ACRs)
3. Solar energetic particles (SEPs)
4. Particles accelerated by SIRs or CIRs
5. Energetic particles accelerated in planetary magnetospheres.

The study of these particle populations at different latitudes and under different heliospheric conditions provides information about:

- the global structure of the heliosphere during solar minimum and solar maximum conditions
- the mechanisms of particle propagation in the heliosphere
- properties of solar source regions (charge states, composition).

Energetic particles given insight both on the heliosphere and on processes back at Sun.

Particle studies combine three aspects: origin/acceleration, propagation, detection.

The study of these particle populations at different latitudes and under different heliospheric conditions provides information about:

- the global structure of the heliosphere during solar minimum and solar maximum conditions
- the mechanisms of particle propagation in the heliosphere
- properties of solar source regions (charge states, composition).

Energetic particles given insight both on the heliosphere and on processes back at Sun.

Particle studies combine three aspects: origin/acceleration, propagation, detection.

The study of these particle populations at different latitudes and under different heliospheric conditions provides information about:

- the global structure of the heliosphere during solar minimum and solar maximum conditions
- the mechanisms of particle propagation in the heliosphere
- properties of solar source regions (charge states, composition).

Energetic particles given insight both on the heliosphere and on processes back at Sun.

Particle studies combine three aspects: origin/acceleration, propagation, detection.

The study of these particle populations at different latitudes and under different heliospheric conditions provides information about:

- the global structure of the heliosphere during solar minimum and solar maximum conditions
- the mechanisms of particle propagation in the heliosphere
- **properties of solar source regions (charge states, composition).**

Energetic particles given insight both on the heliosphere and on processes back at Sun.

Particle studies combine three aspects: origin/acceleration, propagation, detection.

The study of these particle populations at different latitudes and under different heliospheric conditions provides information about:

- the global structure of the heliosphere during solar minimum and solar maximum conditions
- the mechanisms of particle propagation in the heliosphere
- properties of solar source regions (charge states, composition).

Energetic particles given insight both on the heliosphere and on processes back at Sun.

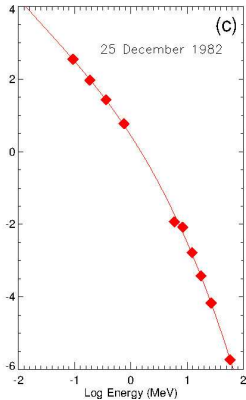
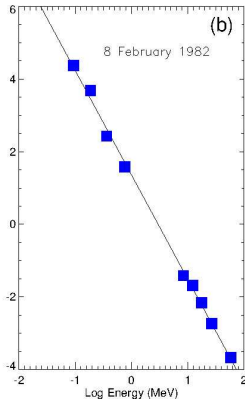
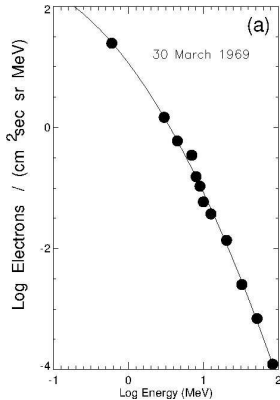
Particle studies combine three aspects: origin/acceleration, propagation, detection.

The study of these particle populations at different latitudes and under different heliospheric conditions provides information about:

- the global structure of the heliosphere during solar minimum and solar maximum conditions
- the mechanisms of particle propagation in the heliosphere
- properties of solar source regions (charge states, composition).

Energetic particles given insight both on the heliosphere and on processes back at Sun.

Particle studies combine three aspects: origin/acceleration, propagation, detection.



Interplanetary electron spectra for events extending to ~ 100 MeV. After Moses et al, 1989.

How do kinetic energies relate to the particle velocity?

Proton mass: 938 MeV

Electron mass: 511 KeV

From these, if energies are given in eV units, velocities can be readily deduced as a fraction of the speed of light.

What is the velocity of a 100 MeV electron? And a 100 MeV proton?

$$E = \frac{m_0}{\sqrt{1 - (v/c)^2}} - m_0$$

$$v/c = \sqrt{1 - 1/(E/m_0 + 1)^2}$$

what is the energy of an electron with $v/c = 1/3$? And a ion with $v/c = 0.1$?

How do kinetic energies relate to the particle velocity?

Proton mass: 938 MeV

Electron mass: 511 KeV

From these, if energies are given in eV units, velocities can be readily deduced as a fraction of the speed of light.

What is the velocity of a 100 MeV electron? And a 100 MeV proton?

$$E = \frac{m_0}{\sqrt{1 - (v/c)^2}} - m_0$$

$$v/c = \sqrt{1 - 1/(E/m_0 + 1)^2}$$

what is the energy of an electron with $v/c = 1/3$? And a ion with $v/c = 0.1$?

How do kinetic energies relate to the particle velocity?

Proton mass: 938 MeV

Electron mass: 511 KeV

From these, if energies are given in eV units, velocities can be readily deduced as a fraction of the speed of light.

What is the velocity of a 100 MeV electron? And a 100 MeV proton?

$$E = \frac{m_0}{\sqrt{1 - (v/c)^2}} - m_0$$

$$v/c = \sqrt{1 - 1/(E/m_0 + 1)^2}$$

what is the energy of an electron with $v/c = 1/3$? And a ion with $v/c = 0.1$?

How do kinetic energies relate to the particle velocity?

Proton mass: 938 MeV

Electron mass: 511 KeV

From these, if energies are given in eV units, velocities can be readily deduced as a fraction of the speed of light.

What is the velocity of a 100 MeV electron? And a 100 MeV proton?

$$E = \frac{m_0}{\sqrt{1 - (v/c)^2}} - m_0$$

$$v/c = \sqrt{1 - 1/(E/m_0 + 1)^2}$$

what is the energy of an electron with $v/c = 1/3$? And a ion with $v/c = 0.1$?

How do kinetic energies relate to the particle velocity?

Proton mass: 938 MeV

Electron mass: 511 KeV

From these, if energies are given in eV units, velocities can be readily deduced as a fraction of the speed of light.

What is the velocity of a 100 MeV electron? And a 100 MeV proton?

$$E = \frac{m_0}{\sqrt{1 - (v/c)^2}} - m_0$$

$$v/c = \sqrt{1 - 1/(E/m_0 + 1)^2}$$

what is the energy of an electron with $v/c = 1/3$? And a ion with $v/c = 0.1$?

How do kinetic energies relate to the particle velocity?

Proton mass: 938 MeV

Electron mass: 511 KeV

From these, if energies are given in eV units, velocities can be readily deduced as a fraction of the speed of light.

What is the velocity of a 100 MeV electron? And a 100 MeV proton?

$$E = \frac{m_0}{\sqrt{1 - (v/c)^2}} - m_0$$

$$v/c = \sqrt{1 - 1/(E/m_0 + 1)^2}$$

what is the energy of an electron with $v/c = 1/3$? And a ion with $v/c = 0.1$?

How do kinetic energies relate to the particle velocity?

Proton mass: 938 MeV

Electron mass: 511 KeV

From these, if energies are given in eV units, velocities can be readily deduced as a fraction of the speed of light.

What is the velocity of a 100 MeV electron? And a 100 MeV proton?

$$E = \frac{m_0}{\sqrt{1 - (v/c)^2}} - m_0$$

$$v/c = \sqrt{1 - 1/(E/m_0 + 1)^2}$$

what is the energy of an electron with $v/c = 1/3$? And a ion with $v/c = 0.1$?

How do kinetic energies relate to the particle velocity?

Proton mass: 938 MeV

Electron mass: 511 KeV

From these, if energies are given in eV units, velocities can be readily deduced as a fraction of the speed of light.

What is the velocity of a 100 MeV electron? And a 100 MeV proton?

$$E = \frac{m_0}{\sqrt{1 - (v/c)^2}} - m_0$$

$$v/c = \sqrt{1 - 1/(E/m_0 + 1)^2}$$

what is the energy of an electron with $v/c = 1/3$? And a ion with $v/c = 0.1$?

How do kinetic energies relate to the particle velocity?

Proton mass: 938 MeV

Electron mass: 511 KeV

From these, if energies are given in eV units, velocities can be readily deduced as a fraction of the speed of light.

What is the velocity of a 100 MeV electron? And a 100 MeV proton?

$$E = \frac{m_0}{\sqrt{1 - (v/c)^2}} - m_0$$

$$v/c = \sqrt{1 - 1/(E/m_0 + 1)^2}$$

what is the energy of an electron with $v/c = 1/3$? And a ion with $v/c = 0.1$?

What about rigidity?

Rigidity is essentially momentum over charge and the energy used is GV.

For protons, with units for energy and mass in eV type units

$$E_k = E - m_0$$

$$E^2 = m_0^2 + P^2$$

Exercise: derive the relation between Kinetic energy and rigidity for protons. What is the kinetic energy of a proton with rigidity 10 GV, and for 1 GV?

What is the rigidity for a proton with $v/c = 0.9$? And a proton with $v/c = 0.1$?

What about rigidity?

Rigidity is essentially momentum over charge and the energy used is GV.

For protons, with units for energy and mass in eV type units

$$E_k = E - m_0$$

$$E^2 = m_0^2 + P^2$$

Exercise: derive the relation between Kinetic energy and rigidity for protons. What is the kinetic energy of a protons with rigidity 10 GV, and for 1 GV?

What is the rigidity for a proton with $v/c = 0.9$? And a proton with $v/c = 0.1$?

What about rigidity?

Rigidity is essentially momentum over charge and the energy used is GV.

For protons, with units for energy and mass in eV type units

$$E_k = E - m_0$$

$$E^2 = m_0^2 + P^2$$

Exercise: derive the relation between Kinetic energy and rigidity for protons. What is the kinetic energy of a proton with rigidity 10 GV, and for 1 GV?

What is the rigidity for a proton with $v/c = 0.9$? And a proton with $v/c = 0.1$?

What about rigidity?

Rigidity is essentially momentum over charge and the energy used is GV.

For protons, with units for energy and mass in eV type units

$$E_k = E - m_0$$

$$E^2 = m_0^2 + P^2$$

Exercise: derive the relation between Kinetic energy and rigidity for protons. What is the kinetic energy of a proton with rigidity 10 GV, and for 1 GV?

What is the rigidity for a proton with $v/c = 0.9$? And a proton with $v/c = 0.1$?

What about rigidity?

Rigidity is essentially momentum over charge and the energy used is GV.

For protons, with units for energy and mass in eV type units

$$E_k = E - m_0$$

$$E^2 = m_0^2 + P^2$$

Exercise: derive the relation between Kinetic energy and rigidity for protons. What is the kinetic energy of a proton with rigidity 10 GV, and for 1 GV?

What is the rigidity for a proton with $v/c = 0.9$? And a proton with $v/c = 0.1$?

What about rigidity?

Rigidity is essentially momentum over charge and the energy used is GV.

For protons, with units for energy and mass in eV type units

$$E_k = E - m_0$$

$$E^2 = m_0^2 + P^2$$

Exercise: derive the relation between Kinetic energy and rigidity for protons. What is the kinetic energy of a proton with rigidity 10 GV, and for 1 GV?

What is the rigidity for a proton with $v/c = 0.9$? And a proton with $v/c = 0.1$?

What about rigidity?

Rigidity is essentially momentum over charge and the energy used is GV.

For protons, with units for energy and mass in eV type units

$$E_k = E - m_0$$

$$E^2 = m_0^2 + P^2$$

Exercise: derive the relation between Kinetic energy and rigidity for protons. What is the kinetic energy of a protons with rigidity 10 GV, and for 1 GV?

What is the rigidity for a proton with $v/c = 0.9$? And a proton with $v/c = 0.1$?

What about rigidity?

Rigidity is essentially momentum over charge and the energy used is GV.

For protons, with units for energy and mass in eV type units

$$E_k = E - m_0$$

$$E^2 = m_0^2 + P^2$$

Exercise: derive the relation between Kinetic energy and rigidity for protons. What is the kinetic energy of a proton with rigidity 10 GV, and for 1 GV?

What is the rigidity for a proton with $v/c = 0.9$? And a proton with $v/c = 0.1$?

Source regions of ions

Observations of source regions can be taken literally to mean the sites on the Sun where enhanced accelerated ions, including heavy elements can be seen, something possible through spectral observations in γ -rays.

Those can provide information on the energy spectrum of the accelerated ions very close to the solar surface, and on the composition of the ambient atmosphere and the accelerated ions.

This kind of direct remote observations are rare, most of the photons which give us remote observations of energetic processes at the Sun result from either thermal emission from the heated plasma or are produced by non-thermal electrons.

Generally the term source region refers to a region on the Sun undergoing relevant changes at the time when the ions observed in situ were expected to have left the Sun, that is, the identification relies essentially in temporal associations, not on remote signatures of accelerated ions.

Source regions of ions

Observations of source regions can be taken literally to mean the sites on the Sun where enhanced accelerated ions, including heavy elements can be seen, something possible through spectral observations in γ -rays.

Those can provide information on the energy spectrum of the accelerated ions very close to the solar surface, and on the composition of the ambient atmosphere and the accelerated ions.

This kind of direct remote observations are rare, most of the photons which give us remote observations of energetic processes at the Sun result from either thermal emission from the heated plasma or are produced by non-thermal electrons.

Generally the term source region refers to a region on the Sun undergoing relevant changes at the time when the ions observed in situ were expected to have left the Sun, that is, the identification relies essentially in temporal associations, not on remote signatures of accelerated ions.

Source regions of ions

Observations of source regions can be taken literally to mean the sites on the Sun where enhanced accelerated ions, including heavy elements can be seen, something possible through spectral observations in γ -rays.

Those can provide information on the energy spectrum of the accelerated ions very close to the solar surface, and on the composition of the ambient atmosphere and the accelerated ions.

This kind of direct remote observations are rare, most of the photons which give us remote observations of energetic processes at the Sun result from either thermal emission from the heated plasma or are produced by non-thermal electrons.

Generally the term source region refers to a region on the Sun undergoing relevant changes at the time when the ions observed in situ were expected to have left the Sun, that is, the identification relies essentially in temporal associations, not on remote signatures of accelerated ions.

Source regions of ions

Observations of source regions can be taken literally to mean the sites on the Sun where enhanced accelerated ions, including heavy elements can be seen, something possible through spectral observations in γ -rays.

Those can provide information on the energy spectrum of the accelerated ions very close to the solar surface, and on the composition of the ambient atmosphere and the accelerated ions.

This kind of direct remote observations are rare, most of the photons which give us remote observations of energetic processes at the Sun result from either thermal emission from the heated plasma or are produced by non-thermal electrons.

Generally the term source region refers to a region on the Sun undergoing relevant changes at the time when the ions observed in situ were expected to have left the Sun, that is, the identification relies essentially in temporal associations, not on remote signatures of accelerated ions.

Source regions of ions

Observations of source regions can be taken literally to mean the sites on the Sun where enhanced accelerated ions, including heavy elements can be seen, something possible through spectral observations in γ -rays.

Those can provide information on the energy spectrum of the accelerated ions very close to the solar surface, and on the composition of the ambient atmosphere and the accelerated ions.

This kind of direct remote observations are rare, most of the photons which give us remote observations of energetic processes at the Sun result from either thermal emission from the heated plasma or are produced by non-thermal electrons.

Generally the term source region refers to a region on the Sun undergoing relevant changes at the time when the ions observed in situ were expected to have left the Sun, that is, the identification relies essentially in temporal associations, not on remote signatures of accelerated ions.

Remote ion observations

When energetic ions, accelerated in flare processes, collide with the solar atmosphere, they produce excited nuclei, as well as secondary neutrons and positrons, and π -mesons.

These then produce observable signatures, namely γ -ray emission via secondary processes.

The gamma-ray line emission produced by accelerated ions consists of narrow lines, resulting from the interaction of accelerated protons and α -particles with ambient heavy nuclei.

It includes also broad lines, produced by the inverse reactions between the accelerated heavy nuclei and the ambient hydrogen and helium.

The γ -ray line spectrum, in particular the nuclear deexcitation lines, their intensities, shapes and time histories, convey information about the accelerated ions responsible for their production, and acceleration parameters.

Remote ion observations

When energetic ions, accelerated in flare processes, collide with the solar atmosphere, they produce excited nuclei, as well as secondary neutrons and positrons, and π -mesons.

These then produce observable signatures, namely γ -ray emission via secondary processes.

The gamma-ray line emission produced by accelerated ions consists of narrow lines, resulting from the interaction of accelerated protons and α -particles with ambient heavy nuclei.

It includes also broad lines, produced by the inverse reactions between the accelerated heavy nuclei and the ambient hydrogen and helium.

The γ -ray line spectrum, in particular the nuclear deexcitation lines, their intensities, shapes and time histories, convey information about the accelerated ions responsible for their production, and acceleration parameters.

Remote ion observations

When energetic ions, accelerated in flare processes, collide with the solar atmosphere, they produce excited nuclei, as well as secondary neutrons and positrons, and π -mesons.

These then produce observable signatures, namely γ -ray emission via secondary processes.

The gamma-ray line emission produced by accelerated ions consists of narrow lines, resulting from the interaction of accelerated protons and α -particles with ambient heavy nuclei.

It includes also broad lines, produced by the inverse reactions between the accelerated heavy nuclei and the ambient hydrogen and helium.

The γ -ray line spectrum, in particular the nuclear deexcitation lines, their intensities, shapes and time histories, convey information about the accelerated ions responsible for their production, and acceleration parameters.

Remote ion observations

When energetic ions, accelerated in flare processes, collide with the solar atmosphere, they produce excited nuclei, as well as secondary neutrons and positrons, and π -mesons.

These then produce observable signatures, namely γ -ray emission via secondary processes.

The gamma-ray line emission produced by accelerated ions consists of narrow lines, resulting from the interaction of accelerated protons and α -particles with ambient heavy nuclei.

It includes also broad lines, produced by the inverse reactions between the accelerated heavy nuclei and the ambient hydrogen and helium.

The γ -ray line spectrum, in particular the nuclear deexcitation lines, their intensities, shapes and time histories, convey information about the accelerated ions responsible for their production, and acceleration parameters.

Remote ion observations

When energetic ions, accelerated in flare processes, collide with the solar atmosphere, they produce excited nuclei, as well as secondary neutrons and positrons, and π -mesons.

These then produce observable signatures, namely γ -ray emission via secondary processes.

The gamma-ray line emission produced by accelerated ions consists of narrow lines, resulting from the interaction of accelerated protons and α -particles with ambient heavy nuclei.

It includes also broad lines, produced by the inverse reactions between the accelerated heavy nuclei and the ambient hydrogen and helium.

The γ -ray line spectrum, in particular the nuclear deexcitation lines, their intensities, shapes and time histories, convey information about the accelerated ions responsible for their production, and acceleration parameters.

Remote ion observations

When energetic ions, accelerated in flare processes, collide with the solar atmosphere, they produce excited nuclei, as well as secondary neutrons and positrons, and π -mesons.

These then produce observable signatures, namely γ -ray emission via secondary processes.

The gamma-ray line emission produced by accelerated ions consists of narrow lines, resulting from the interaction of accelerated protons and α -particles with ambient heavy nuclei.

It includes also broad lines, produced by the inverse reactions between the accelerated heavy nuclei and the ambient hydrogen and helium.

The γ -ray line spectrum, in particular the nuclear deexcitation lines, their intensities, shapes and time histories, convey information about the accelerated ions responsible for their production, and acceleration parameters.

Remote ion observations

This aspect of high-energy flare emission has been well explored in the past and for example it is now established a near energy equivalency of accelerated ions and electrons in flares.

It is known for some time, from the analysis of broad gamma-ray lines in flares, that there are significant enhancements in the accelerated α to proton ratio, and also in Fe and other heavy elements.

Gamma-ray spectroscopy was also able, in recent years, to determine the ^3He to ^4He ratio in flares.

Mandzhavidze and Ramaty (2000) were able to show that 7 out of 20 flares had enhancements in $^3\text{He}/^4\text{He} > 0.1$ and in some cases $^3\text{He}/^4\text{He} \sim 1$.

The $^3\text{He}/^4\text{He}$ values in the remaining flares had large uncertainties, but they were consistent with $^3\text{He}/^4\text{He} \sim 1$ being ≥ 0.1 in all cases.

γ -ray spectroscopy thus suggest that ^3He is significantly enhanced in γ -ray line flares.

Remote ion observations

This aspect of high-energy flare emission has been well explored in the past and for example it is now established a near energy equivalency of accelerated ions and electrons in flares.

It is known for some time, from the analysis of broad gamma-ray lines in flares, that there are significant enhancements in the accelerated α to proton ratio, and also in Fe and other heavy elements.

Gamma-ray spectroscopy was also able, in recent years, to determine the ^3He to ^4He ratio in flares.

Mandzhavidze and Ramaty (2000) were able to show that 7 out of 20 flares had enhancements in $^3\text{He}/^4\text{He} > 0.1$ and in some cases $^3\text{He}/^4\text{He} \sim 1$.

The $^3\text{He}/^4\text{He}$ values in the remaining flares had large uncertainties, but they were consistent with $^3\text{He}/^4\text{He} \sim 1$ being ≥ 0.1 in all cases.

γ -ray spectroscopy thus suggest that ^3He is significantly enhanced in γ -ray line flares.

Remote ion observations

This aspect of high-energy flare emission has been well explored in the past and for example it is now established a near energy equivalency of accelerated ions and electrons in flares.

It is known for some time, from the analysis of broad gamma-ray lines in flares, that there are significant enhancements in the accelerated α to proton ratio, and also in Fe and other heavy elements.

Gamma-ray spectroscopy was also able, in recent years, to determine the ^3He to ^4He ratio in flares.

Mandzhavidze and Ramaty (2000) were able to show that 7 out of 20 flares had enhancements in $^3\text{He}/^4\text{He} > 0.1$ and in some cases $^3\text{He}/^4\text{He} \sim 1$.

The $^3\text{He}/^4\text{He}$ values in the remaining flares had large uncertainties, but they were consistent with $^3\text{He}/^4\text{He} \sim 1$ being ≥ 0.1 in all cases.

γ -ray spectroscopy thus suggest that ^3He is significantly enhanced in γ -ray line flares.

Remote ion observations

This aspect of high-energy flare emission has been well explored in the past and for example it is now established a near energy equivalency of accelerated ions and electrons in flares.

It is known for some time, from the analysis of broad gamma-ray lines in flares, that there are significant enhancements in the accelerated α to proton ratio, and also in Fe and other heavy elements.

Gamma-ray spectroscopy was also able, in recent years, to determine the ^3He to ^4He ratio in flares.

Mandzhavidze and Ramaty (2000) were able to show that 7 out of 20 flares had enhancements in $^3\text{He}/^4\text{He} > 0.1$ and in some cases $^3\text{He}/^4\text{He} \sim 1$.

The $^3\text{He}/^4\text{He}$ values in the remaining flares had large uncertainties, but they were consistent with $^3\text{He}/^4\text{He} \sim 1$ being ≥ 0.1 in all cases.

γ -ray spectroscopy thus suggest that ^3He is significantly enhanced in γ -ray line flares.

Remote ion observations

This aspect of high-energy flare emission has been well explored in the past and for example it is now established a near energy equivalency of accelerated ions and electrons in flares.

It is known for some time, from the analysis of broad gamma-ray lines in flares, that there are significant enhancements in the accelerated α to proton ratio, and also in Fe and other heavy elements.

Gamma-ray spectroscopy was also able, in recent years, to determine the ^3He to ^4He ratio in flares.

Mandzhavidze and Ramaty (2000) were able to show that 7 out of 20 flares had enhancements in $^3\text{He}/^4\text{He} > 0.1$ and in some cases $^3\text{He}/^4\text{He} \sim 1$.

The $^3\text{He}/^4\text{He}$ values in the remaining flares had large uncertainties, but they were consistent with $^3\text{He}/^4\text{He} \sim 1$ being ≥ 0.1 in all cases.

γ -ray spectroscopy thus suggest that ^3He is significantly enhanced in γ -ray line flares.

Remote ion observations

This aspect of high-energy flare emission has been well explored in the past and for example it is now established a near energy equivalency of accelerated ions and electrons in flares.

It is known for some time, from the analysis of broad gamma-ray lines in flares, that there are significant enhancements in the accelerated α to proton ratio, and also in Fe and other heavy elements.

Gamma-ray spectroscopy was also able, in recent years, to determine the ^3He to ^4He ratio in flares.

Mandzhavidze and Ramaty (2000) were able to show that 7 out of 20 flares had enhancements in $^3\text{He}/^4\text{He} > 0.1$ and in some cases $^3\text{He}/^4\text{He} \sim 1$.

The $^3\text{He}/^4\text{He}$ values in the remaining flares had large uncertainties, but they were consistent with $^3\text{He}/^4\text{He} \sim 1$ being ≥ 0.1 in all cases.

γ -ray spectroscopy thus suggest that ^3He is significantly enhanced in γ -ray line flares.

Remote ion observations

This aspect of high-energy flare emission has been well explored in the past and for example it is now established a near energy equivalency of accelerated ions and electrons in flares.

It is known for some time, from the analysis of broad gamma-ray lines in flares, that there are significant enhancements in the accelerated α to proton ratio, and also in Fe and other heavy elements.

Gamma-ray spectroscopy was also able, in recent years, to determine the ^3He to ^4He ratio in flares.

Mandzhavidze and Ramaty (2000) were able to show that 7 out of 20 flares had enhancements in $^3\text{He}/^4\text{He} > 0.1$ and in some cases $^3\text{He}/^4\text{He} \sim 1$.

The $^3\text{He}/^4\text{He}$ values in the remaining flares had large uncertainties, but they were consistent with $^3\text{He}/^4\text{He} \sim 1$ being ≥ 0.1 in all cases.

γ -ray spectroscopy thus suggest that ^3He is significantly enhanced in γ -ray line flares.

Remote ion observations

Although spectroscopic ion observations have been available for relatively some time, the location, size and geometry of the ion collision regions remained unknown until recently.

This issue could only be tackled with the launch of the NASA Reuven Ramaty High Energy Solar Spectroscopic Imager (RHESSI) mission on February 5, 2002.

RHESSI provides high resolution imaging and spectroscopy from soft X-rays (3 keV) to γ -rays (17 MeV) for solar measurements.

Vestrand and Forrest (1993) detection of the 2.223 MeV line in an over-the-limb flare event led the authors to suggest that ions would be accelerated by a CME-driven shock.

If that were the case one would expect the ions to be widely dispersed and/or displaced from the flare site, while if they behaved similarly to electrons one would expect footpoint sources located at the flare site.

Remote ion observations

Although spectroscopic ion observations have been available for relatively some time, the location, size and geometry of the ion collision regions remained unknown until recently.

This issue could only be tackled with the launch of the NASA Reuven Ramaty High Energy Solar Spectroscopic Imager (RHESSI) mission on February 5, 2002.

RHESSI provides high resolution imaging and spectroscopy from soft X-rays (3 keV) to γ -rays (17 MeV) for solar measurements.

Vestrand and Forrest (1993) detection of the 2.223 MeV line in an over-the-limb flare event led the authors to suggest that ions would be accelerated by a CME-driven shock.

If that were the case one would expect the ions to be widely dispersed and/or displaced from the flare site, while if they behaved similarly to electrons one would expect footpoint sources located at the flare site.

Remote ion observations

Although spectroscopic ion observations have been available for relatively some time, the location, size and geometry of the ion collision regions remained unknown until recently.

This issue could only be tackled with the launch of the NASA Reuven Ramaty High Energy Solar Spectroscopic Imager (RHESSI) mission on February 5, 2002.

RHESSI provides high resolution imaging and spectroscopy from soft X-rays (3 keV) to γ -rays (17 MeV) for solar measurements.

Vestrand and Forrest (1993) detection of the 2.223 MeV line in an over-the-limb flare event led the authors to suggest that ions would be accelerated by a CME-driven shock.

If that were the case one would expect the ions to be widely dispersed and/or displaced from the flare site, while if they behaved similarly to electrons one would expect footpoint sources located at the flare site.

Remote ion observations

Although spectroscopic ion observations have been available for relatively some time, the location, size and geometry of the ion collision regions remained unknown until recently.

This issue could only be tackled with the launch of the NASA Reuven Ramaty High Energy Solar Spectroscopic Imager (RHESSI) mission on February 5, 2002.

RHESSI provides high resolution imaging and spectroscopy from soft X-rays (3 keV) to γ -rays (17 MeV) for solar measurements.

Vestrand and Forrest (1993) detection of the 2.223 MeV line in an over-the-limb flare event led the authors to suggest that ions would be accelerated by a CME-driven shock.

If that were the case one would expect the ions to be widely dispersed and/or displaced from the flare site, while if they behaved similarly to electrons one would expect footpoint sources located at the flare site.

Remote ion observations

Although spectroscopic ion observations have been available for relatively some time, the location, size and geometry of the ion collision regions remained unknown until recently.

This issue could only be tackled with the launch of the NASA Reuven Ramaty High Energy Solar Spectroscopic Imager (RHESSI) mission on February 5, 2002.

RHESSI provides high resolution imaging and spectroscopy from soft X-rays (3 keV) to γ -rays (17 MeV) for solar measurements.

Vestrand and Forrest (1993) detection of the 2.223 MeV line in an over-the-limb flare event led the authors to suggest that ions would be accelerated by a CME-driven shock.

If that were the case one would expect the ions to be widely dispersed and/or displaced from the flare site, while if they behaved similarly to electrons one would expect footpoint sources located at the flare site.

Remote ion observations

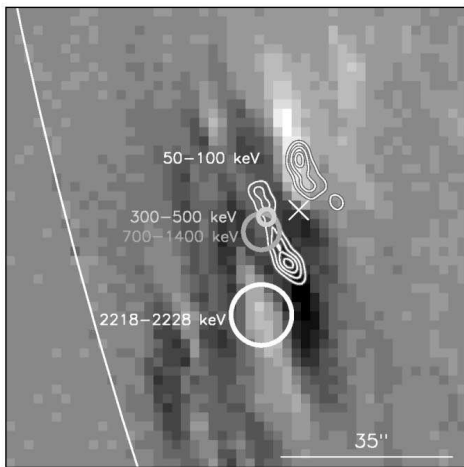
Although spectroscopic ion observations have been available for relatively some time, the location, size and geometry of the ion collision regions remained unknown until recently.

This issue could only be tackled with the launch of the NASA Reuven Ramaty High Energy Solar Spectroscopic Imager (RHESSI) mission on February 5, 2002.

RHESSI provides high resolution imaging and spectroscopy from soft X-rays (3 keV) to γ -rays (17 MeV) for solar measurements.

Vestrand and Forrest (1993) detection of the 2.223 MeV line in an over-the-limb flare event led the authors to suggest that ions would be accelerated by a CME-driven shock.

If that were the case one would expect the ions to be widely dispersed and/or displaced from the flare site, while if they behaved similarly to electrons one would expect footpoint sources located at the flare site.



Circles: 300-500 keV (light gray), 700-1400 keV (dark gray), and 2218-2228 keV (white). Contours: 50-100 keV map. Cross: 50-100 keV emission. Background: SOHO/MDI magnetogram. Krucker et al (2007).

Remote ion observations

The now prevalent view is that gradual SEP events of any energy are due to particle acceleration at the presumed bow shock of a rapid coronal mass ejection and unrelated to the particle acceleration revealed by the γ -ray flare.

There are nonetheless some indications that the some of the gradual events, namely to ones that are well connected magnetically, do show some flare signatures.

RHESSI observations discussed add to these evidence for flare particles inside gradual SEP events. RHESSI has detected γ -ray line emission from three events associated with SEPs detected near 1 AU.

For two of those events, 28 October 2003 and 2 November 2003, it was possible to compute the spectra for the ions at the Sun from the observed narrow line fluences of the 2.223 MeV neutron-capture line and the 4.443 MeV carbon line, and those were compared to power law exponents for the energetic protons observed near 1 AU.

Remote ion observations

The now prevalent view is that gradual SEP events of any energy are due to particle acceleration at the presumed bow shock of a rapid coronal mass ejection and unrelated to the particle acceleration revealed by the γ -ray flare.

There are nonetheless some indications that the some of the gradual events, namely to ones that are well connected magnetically, do show some flare signatures.

RHESSI observations discussed add to these evidence for flare particles inside gradual SEP events. RHESSI has detected γ -ray line emission from three events associated with SEPs detected near 1 AU.

For two of those events, 28 October 2003 and 2 November 2003, it was possible to compute the spectra for the ions at the Sun from the observed narrow line fluences of the 2.223 MeV neutron-capture line and the 4.443 MeV carbon line, and those were compared to power law exponents for the energetic protons observed near 1 AU.

Remote ion observations

The now prevalent view is that gradual SEP events of any energy are due to particle acceleration at the presumed bow shock of a rapid coronal mass ejection and unrelated to the particle acceleration revealed by the γ -ray flare.

There are nonetheless some indications that the some of the gradual events, namely to ones that are well connected magnetically, do show some flare signatures.

RHESSI observations discussed add to these evidence for flare particles inside gradual SEP events. RHESSI has detected γ -ray line emission from three events associated with SEPs detected near 1 AU.

For two of those events, 28 October 2003 and 2 November 2003, it was possible to compute the spectra for the ions at the Sun from the observed narrow line fluences of the 2.223 MeV neutron-capture line and the 4.443 MeV carbon line, and those were compared to power law exponents for the energetic protons observed near 1 AU.

Remote ion observations

The now prevalent view is that gradual SEP events of any energy are due to particle acceleration at the presumed bow shock of a rapid coronal mass ejection and unrelated to the particle acceleration revealed by the γ -ray flare.

There are nonetheless some indications that the some of the gradual events, namely to ones that are well connected magnetically, do show some flare signatures.

RHESSI observations discussed add to these evidence for flare particles inside gradual SEP events. RHESSI has detected γ -ray line emission from three events associated with SEPs detected near 1 AU.

For two of those events, 28 October 2003 and 2 November 2003, it was possible to compute the spectra for the ions at the Sun from the observed narrow line fluences of the 2.223 MeV neutron-capture line and the 4.443 MeV carbon line, and those were compared to power law exponents for the energetic protons observed near 1 AU.

Remote ion observations

The now prevalent view is that gradual SEP events of any energy are due to particle acceleration at the presumed bow shock of a rapid coronal mass ejection and unrelated to the particle acceleration revealed by the γ -ray flare.

There are nonetheless some indications that the some of the gradual events, namely to ones that are well connected magnetically, do show some flare signatures.

RHESSI observations discussed add to these evidence for flare particles inside gradual SEP events. RHESSI has detected γ -ray line emission from three events associated with SEPs detected near 1 AU.

For two of those events, 28 October 2003 and 2 November 2003, it was possible to compute the spectra for the ions at the Sun from the observed narrow line fluences of the 2.223 MeV neutron-capture line and the 4.443 MeV carbon line, and those were compared to power law exponents for the energetic protons observed near 1 AU.

Non-thermal remote electron observations

Electrons interact with the plasmas and magnetic fields in the solar atmosphere to produce hard X-rays through bremsstrahlung collisions, and radio emission through wave particle interactions and synchrotron emission.

These remote signatures can provide precise information on the timing of the particle acceleration event, and information on the plasma conditions in the acceleration or propagation region.

When images are available one can also get direct information on the location and configuration of the acceleration site.

Bremsstrahlung provides quantitative measurements such as spectral information of the HXR producing electrons including total number and energy estimates.

Densities in the corona are generally too low to produce significant HXR emissions, at least to be detected by present-day instrumentation. Most HXR emission therefore is produced in the chromosphere.

Non-thermal remote electron observations

Electrons interact with the plasmas and magnetic fields in the solar atmosphere to produce hard X-rays through bremsstrahlung collisions, and radio emission through wave particle interactions and synchrotron emission.

These remote signatures can provide precise information on the timing of the particle acceleration event, and information on the plasma conditions in the acceleration or propagation region.

When images are available one can also get direct information on the location and configuration of the acceleration site.

Bremsstrahlung provides quantitative measurements such as spectral information of the HXR producing electrons including total number and energy estimates.

Densities in the corona are generally too low to produce significant HXR emissions, at least to be detected by present-day instrumentation. Most HXR emission therefore is produced in the chromosphere.

Non-thermal remote electron observations

Electrons interact with the plasmas and magnetic fields in the solar atmosphere to produce hard X-rays through bremsstrahlung collisions, and radio emission through wave particle interactions and synchrotron emission.

These remote signatures can provide precise information on the timing of the particle acceleration event, and information on the plasma conditions in the acceleration or propagation region.

When images are available one can also get direct information on the location and configuration of the acceleration site.

Bremsstrahlung provides quantitative measurements such as spectral information of the HXR producing electrons including total number and energy estimates.

Densities in the corona are generally too low to produce significant HXR emissions, at least to be detected by present-day instrumentation. Most HXR emission therefore is produced in the chromosphere.

Non-thermal remote electron observations

Electrons interact with the plasmas and magnetic fields in the solar atmosphere to produce hard X-rays through bremsstrahlung collisions, and radio emission through wave particle interactions and synchrotron emission.

These remote signatures can provide precise information on the timing of the particle acceleration event, and information on the plasma conditions in the acceleration or propagation region.

When images are available one can also get direct information on the location and configuration of the acceleration site.

Bremsstrahlung provides quantitative measurements such as spectral information of the HXR producing electrons including total number and energy estimates.

Densities in the corona are generally too low to produce significant HXR emissions, at least to be detected by present-day instrumentation. Most HXR emission therefore is produced in the chromosphere.

Non-thermal remote electron observations

Electrons interact with the plasmas and magnetic fields in the solar atmosphere to produce hard X-rays through bremsstrahlung collisions, and radio emission through wave particle interactions and synchrotron emission.

These remote signatures can provide precise information on the timing of the particle acceleration event, and information on the plasma conditions in the acceleration or propagation region.

When images are available one can also get direct information on the location and configuration of the acceleration site.

Bremsstrahlung provides quantitative measurements such as spectral information of the HXR producing electrons including total number and energy estimates.

Densities in the corona are generally too low to produce significant HXR emissions, at least to be detected by present-day instrumentation. Most HXR emission therefore is produced in the chromosphere.

Non-thermal remote electron observations

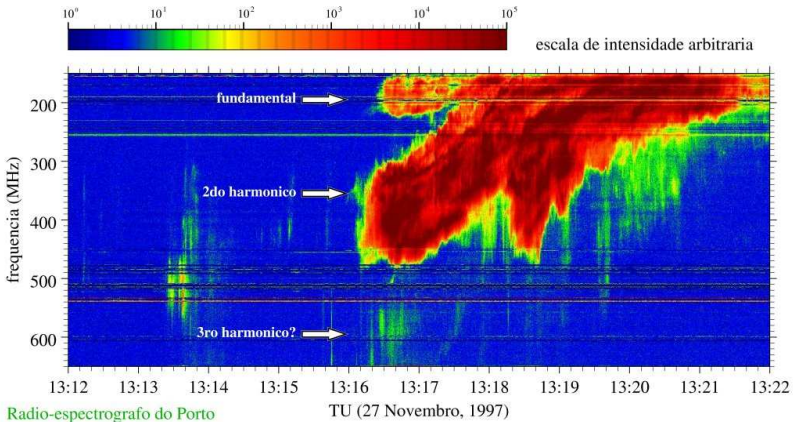
Electrons interact with the plasmas and magnetic fields in the solar atmosphere to produce hard X-rays through bremsstrahlung collisions, and radio emission through wave particle interactions and synchrotron emission.

These remote signatures can provide precise information on the timing of the particle acceleration event, and information on the plasma conditions in the acceleration or propagation region.

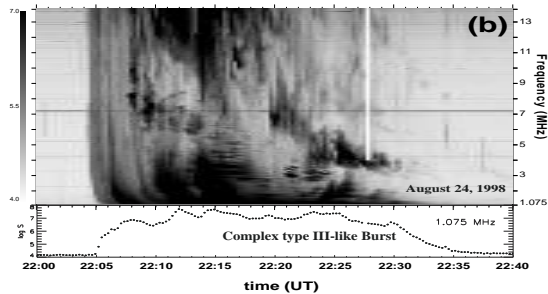
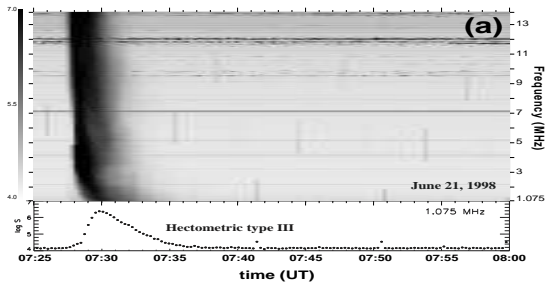
When images are available one can also get direct information on the location and configuration of the acceleration site.

Bremsstrahlung provides quantitative measurements such as spectral information of the HXR producing electrons including total number and energy estimates.

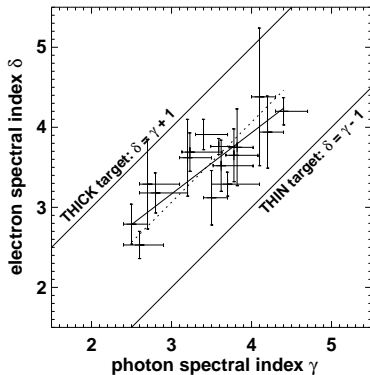
Densities in the corona are generally too low to produce significant HXR emissions, at least to be detected by present-day instrumentation. Most HXR emission therefore is produced in the chromosphere.



Fast drift bursts and a slow-drifting type 2 burst.



The good association of electron events with electron-rich ^3He events suggests that flare electrons reach Earth orbit.

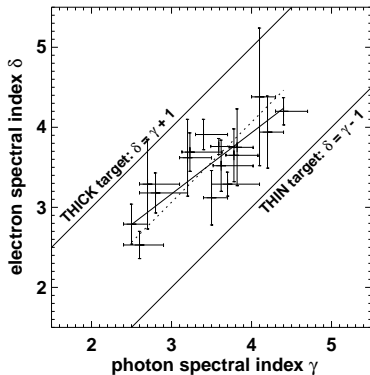


Electron events seen by WIND/3DP with inferred re-release coinciding with HXR emission seen by RHESSI

Good spectral correlation

Only about 1% of flare electrons are released into the IM.

The good association of electron events with electron-rich ^3He events suggests that flare electrons reach Earth orbit.

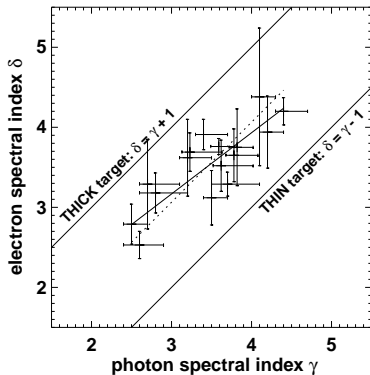


Electron events seen by WIND/3DP with inferred re-release coinciding with HXR emission seen by RHESSI

Good spectral correlation

Only about 1% of flare electrons are released into the IM.

The good association of electron events with electron-rich ^3He events suggests that flare electrons reach Earth orbit.

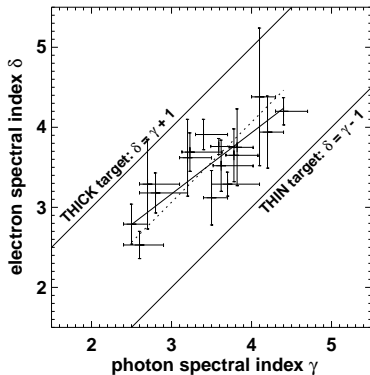


Electron events seen by WIND/3DP with inferred re-release coinciding with HXR emission seen by RHESSI

Good spectral correlation

Only about 1% of flare electrons are released into the IM.

The good association of electron events with electron-rich ${}^3\text{He}$ events suggests that flare electrons reach Earth orbit.

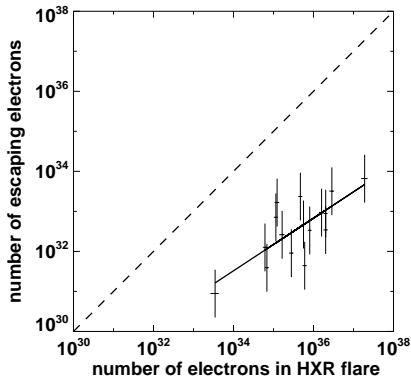


Electron events seen by WIND/3DP with inferred re-release coinciding with HXR emission seen by RHESSI

Good spectral correlation

Only about 1% of flare electrons are released into the IM.

The good association of electron events with electron-rich ${}^3\text{He}$ events suggests that flare electrons reach Earth orbit.

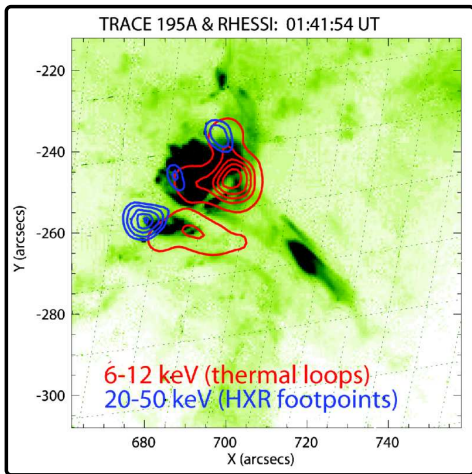


Electron events seen by WIND/3DP with inferred release coinciding with HXR emission seen by RHESSI

Good spectral correlation

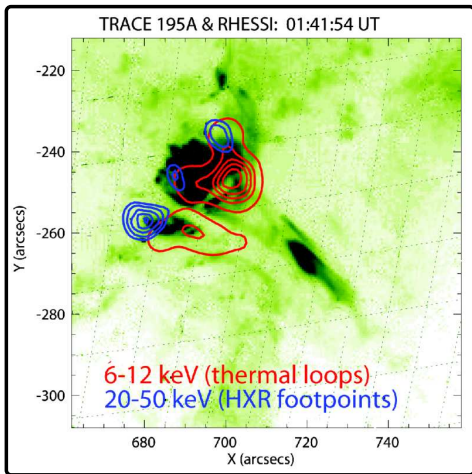
Only about 1% of flare electrons are released into the IM.

Ref: Krucker et al (2007). ApJ 663:L109-L112.



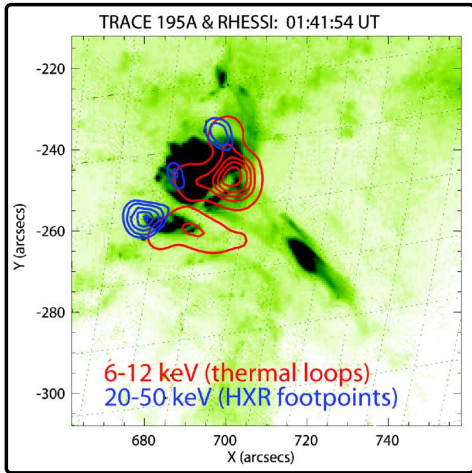
Trace EUV observations of one of Krucker et al (2007) events. Note the EUV jets.

RHESSI contours superposed: thermal loops with HXR footpoints.



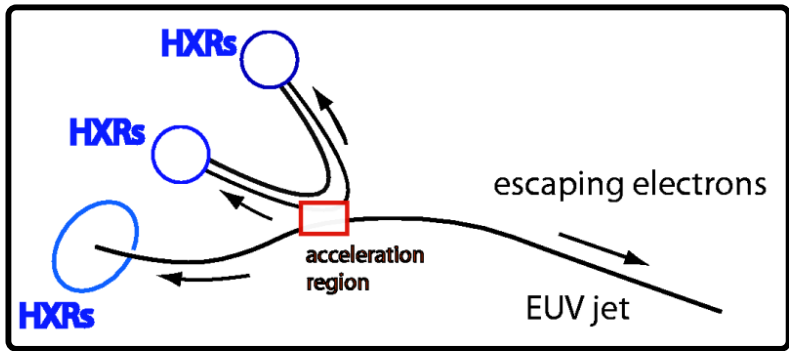
Trace EUV observations of one of Krucker et al (2007) events. Note the EUV jets.

RHESSI contours superposed: thermal loops with HXR footpoints.



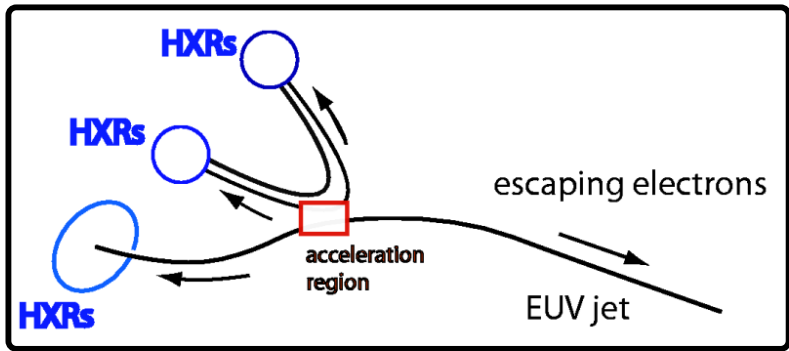
Trace EUV observations of one of Krucker et al (2007) events. Note the EUV jets.

RHESSI contours superposed: thermal loops with HXR footpoints.



Observations suggest simple magnetic reconnection models with newly emerging flux tubes that reconnect with previously open field lines, also known as interchange reconnection.

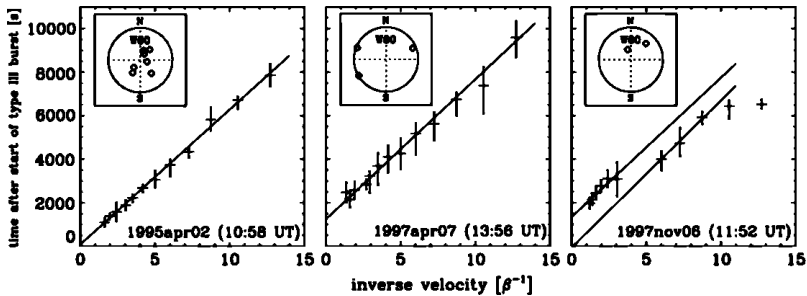
Yet, many in-situ electron events do not agree in time with the HXR burst, and those do not show the same kind of spectral index correlation.



Observations suggest simple magnetic reconnection models with newly emerging flux tubes that reconnect with previously open field lines, also known as interchange reconnection.

Yet, many in-situ electron events do not agree in time with the HXR burst, and those do not show the same kind of spectral index correlation.

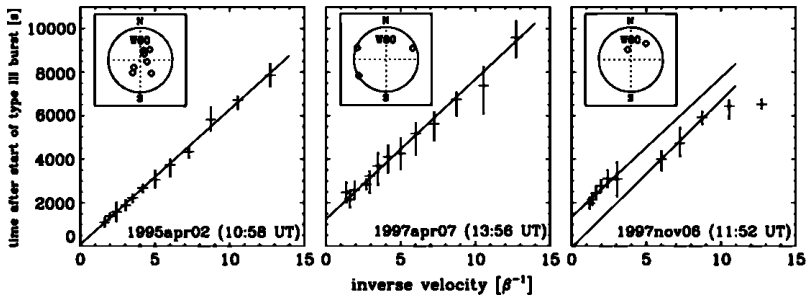
The association between type III bursts and impulsive electron events was revisited in recent years. Krucker et al. (1999), ApJ 519,864.



Inferred release time 100 keV electrons delayed by 10 mn from onset times of type III bursts at frequencies 10 MHz.

Verified also for 79 beam-like events seen by EPAM on ACE. Haggerty and Roelof (2002), ApJ 579, 841-853.

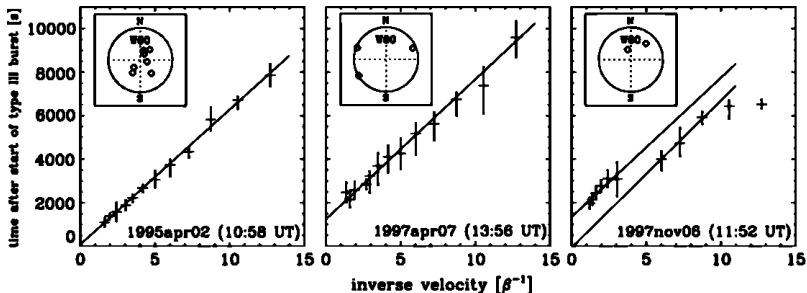
The association between type III bursts and impulsive electron events was revisited in recent years. Krucker et al. (1999), ApJ 519,864.



Inferred release time 100 keV electrons delayed by 10 mn from onset times of type III bursts at frequencies 10 MHz.

Verified also for 79 beam-like events seen by EPAM on ACE. Haggerty and Roelof (2002), ApJ 579, 841-853.

The association between type III bursts and impulsive electron events was revisited in recent years. Krucker et al. (1999), ApJ 519,864.



Inferred release time 100 keV electrons delayed by 10 mn from onset times of type III bursts at frequencies 10 MHz.

Verified also for 79 beam-like events seen by EPAM on ACE. Haggerty and Roelof (2002), ApJ 579, 841-853.